# Supplementary Information

## Enabling isotropic Li growth via Li foil facet-engineering for high-performance Li metal batteries

Yanyan Liu,[a] Shuyue Wang,[a] Minghao Sun,*[b] Min Ling,*[a] Shaodong Zhou*[a] and Chengdu Liang,*[a]

[a.] Zhejiang Provincial Key Laboratory of Advanced Chemical Engineering of Manufacture Technology, College of Chemical and Biochemical Engineering, Zhejiang University, Hangzhou 310027, China
E-mail: minling@zju.edu.cn, szhou@zju.edu.cn, cdliang@zju.edu.cn

[b.] Institute of Zhejiang University-Quzhou, Quzhou 324000, China
E-mail: smhyykzy@163.com

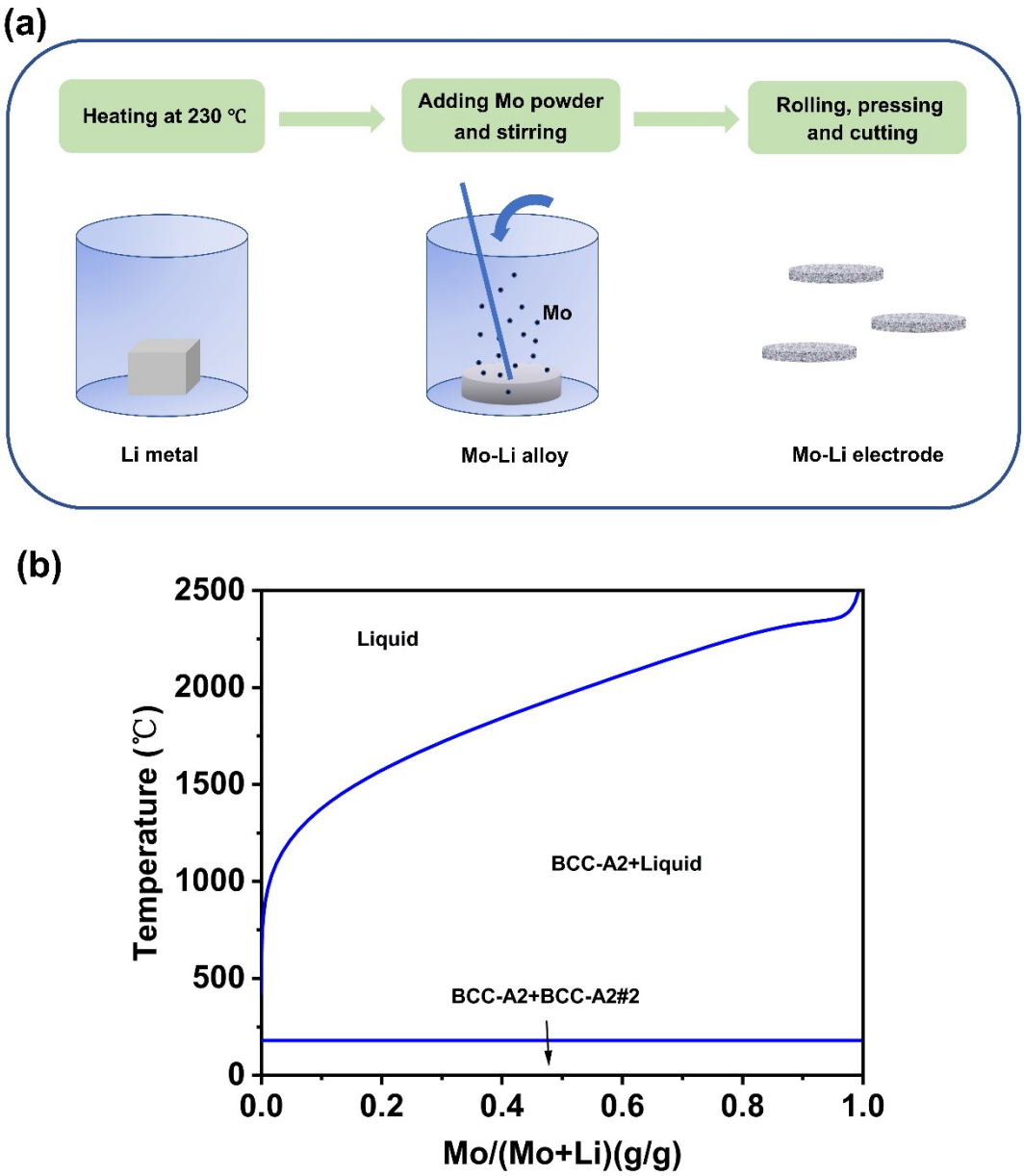


**Figure S1.** (a)Schematic of the fabrication process of Mo-Li electrode; (b) The phase diagram of Mo-Li binary system.`

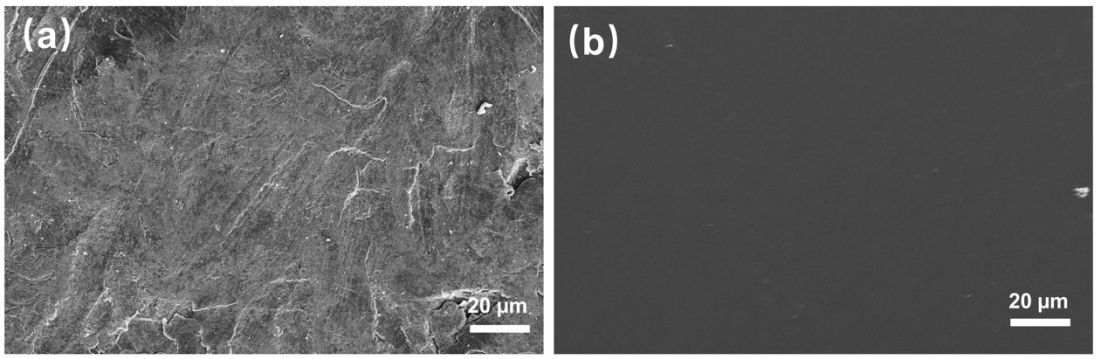


**Figure S2.** SEM images of bare Li (a) and Mo-Li-1 electrode (b). The surface of bare Li was rough and full of natural oxidation products with light contrast. While the surface of Mo-Li electrode was flat and smooth without any oxidation products, showing completely black in the color contrast.

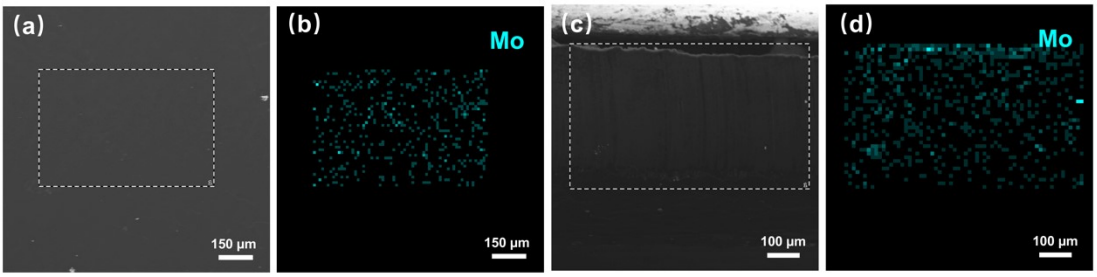


**Figure S3.** EDX mapping results of Mo-Li-1 electrode for the top surface and cross-section. (a) The SEM image of the top surface and its corresponding elemental mapping results (b); (c) The SEM image of the cross-section and its corresponding elemental mapping results (d).

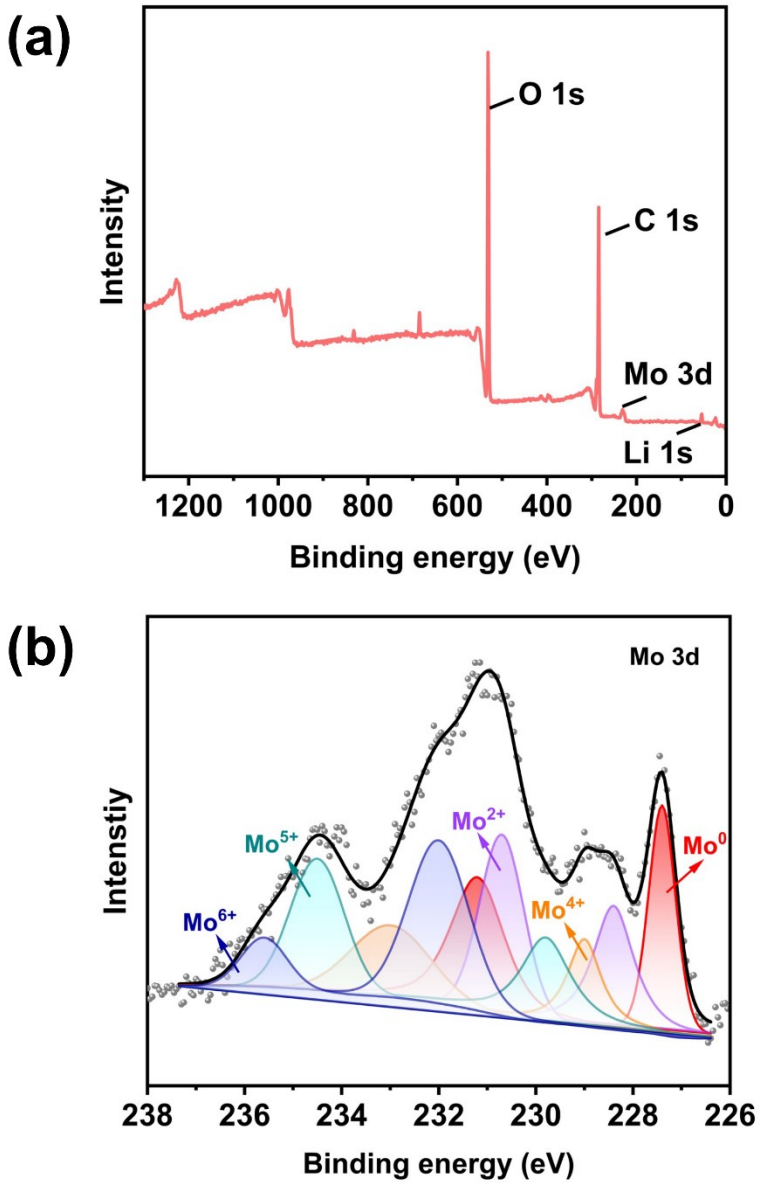


**Figure S4.** XPS spectrum of Mo-Li-1 electrode. (a) Full spectrum; (b) Mo 3d spectrum.

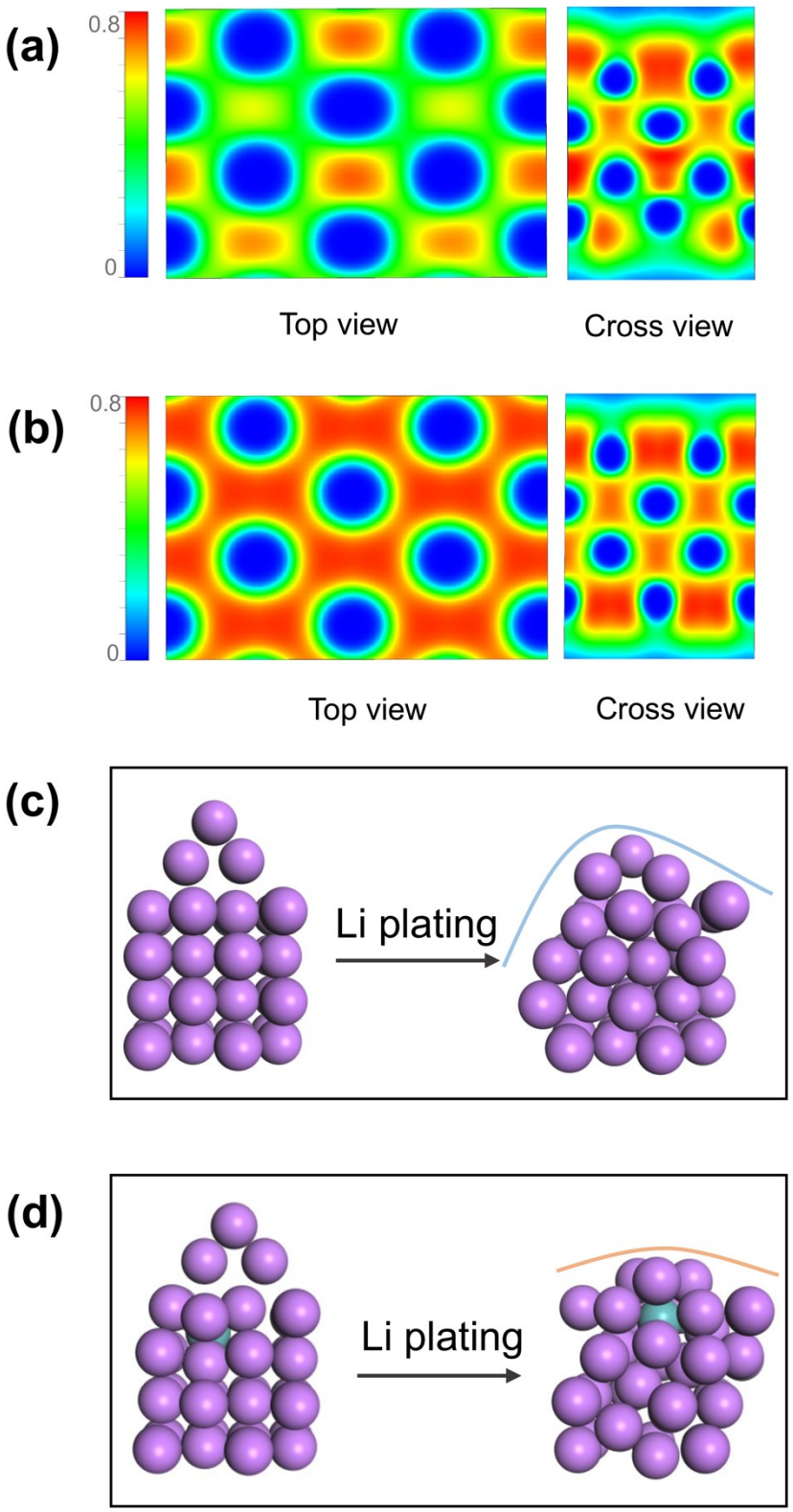


**Figure S5.** ELF results of Li (a) and Mo-Li-1 electrode (b); The deposition of Li cluster on the surface of Li (c) and Mo-Li-1 electrode (d).

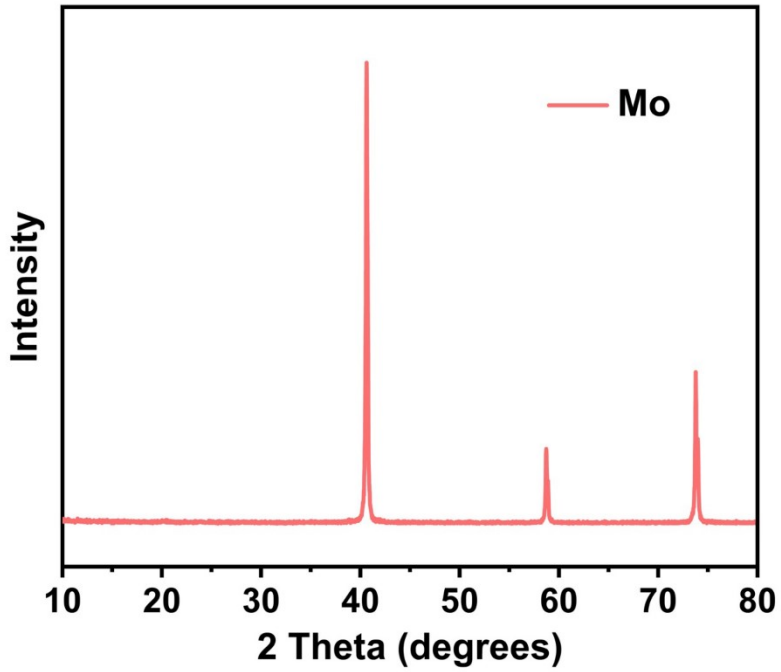


**Figure S6**. The XRD results of Mo powder.

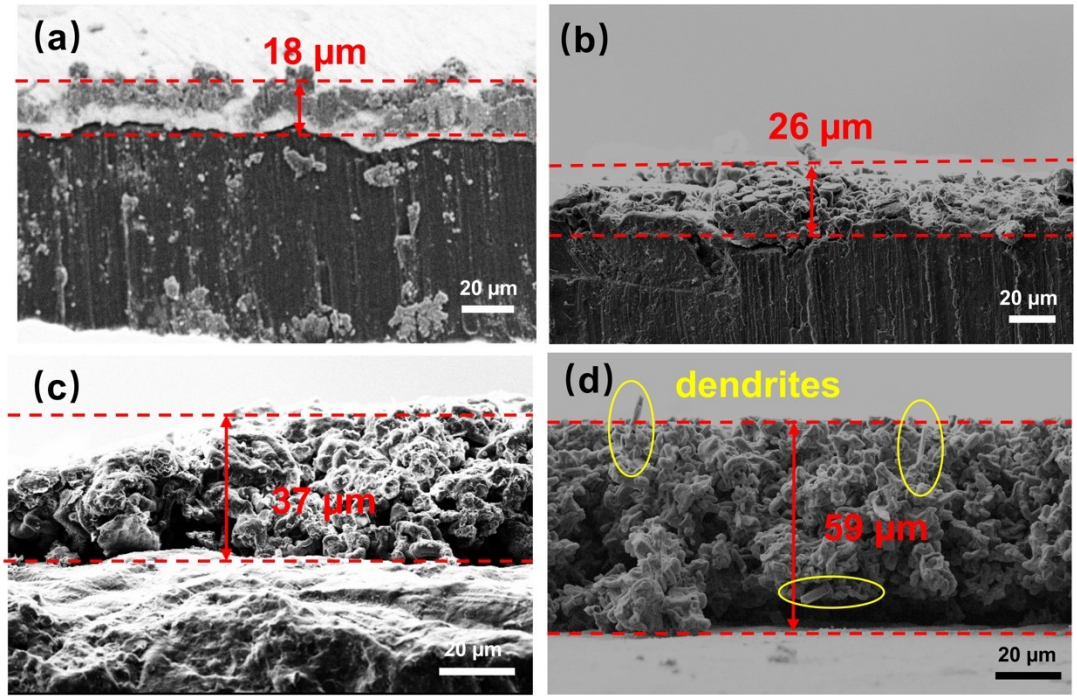


**Figure S7.** The cross-section morphologies of cycled electrodes. (a) Mo-Li-1; (b) Mo-Li-2; (c) Mo-Li-3; (d) bare Li.

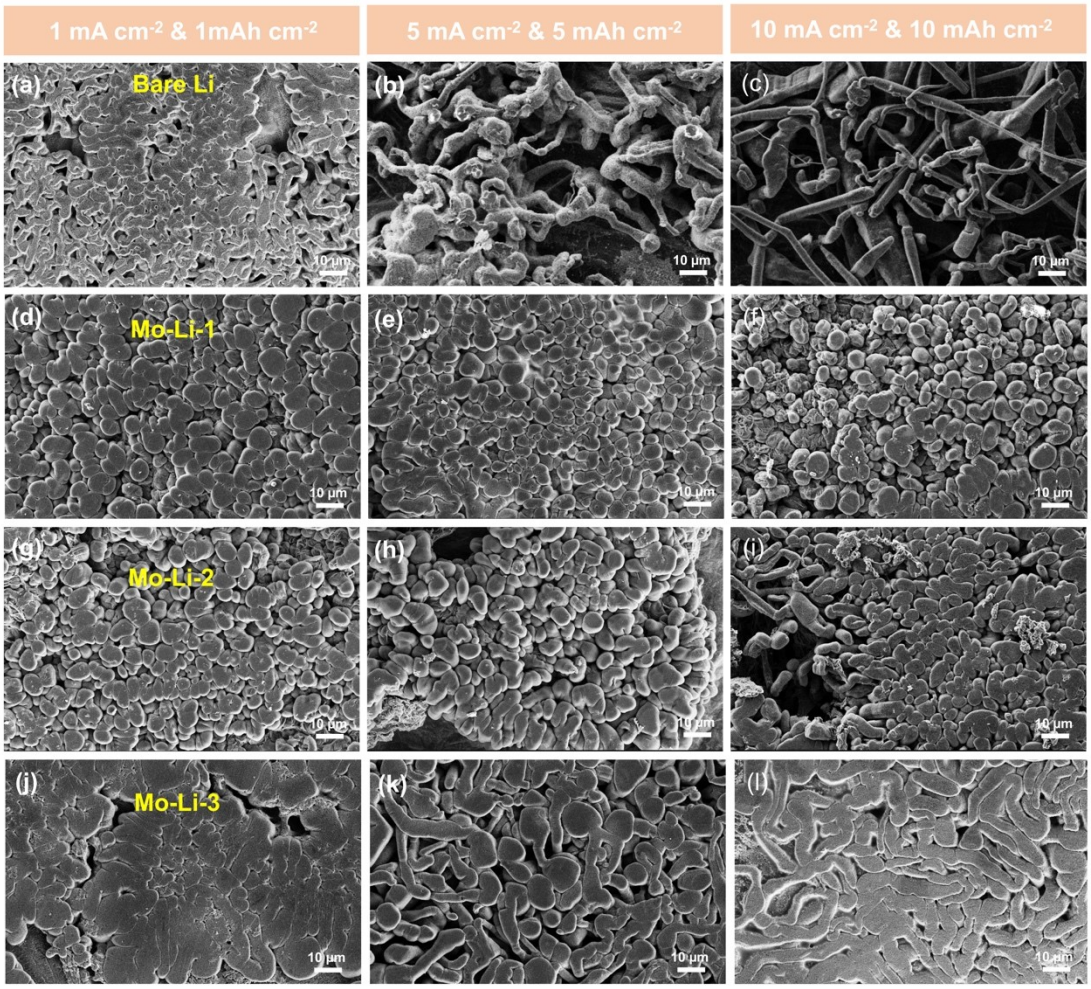


**Figure S8.** The surface morphologies of bare Li (a)-(c), Mo-Li-1(d)-(f), Mo-Li-2(g)-(i), Mo-Li-3(j)- (l) at different current densities. (a), (d), (g), (j) 1 mA $cm^{-2}$ for 1 mAh $cm^{-2}$; (b), (e), (h), (k) 5 mA $cm^{-2}$ for 5 mAh $cm^{-2}$; and (c), (f), (i), (l) 10 mA $cm^{-2}$ for 10 mAh $cm^{-2}$.

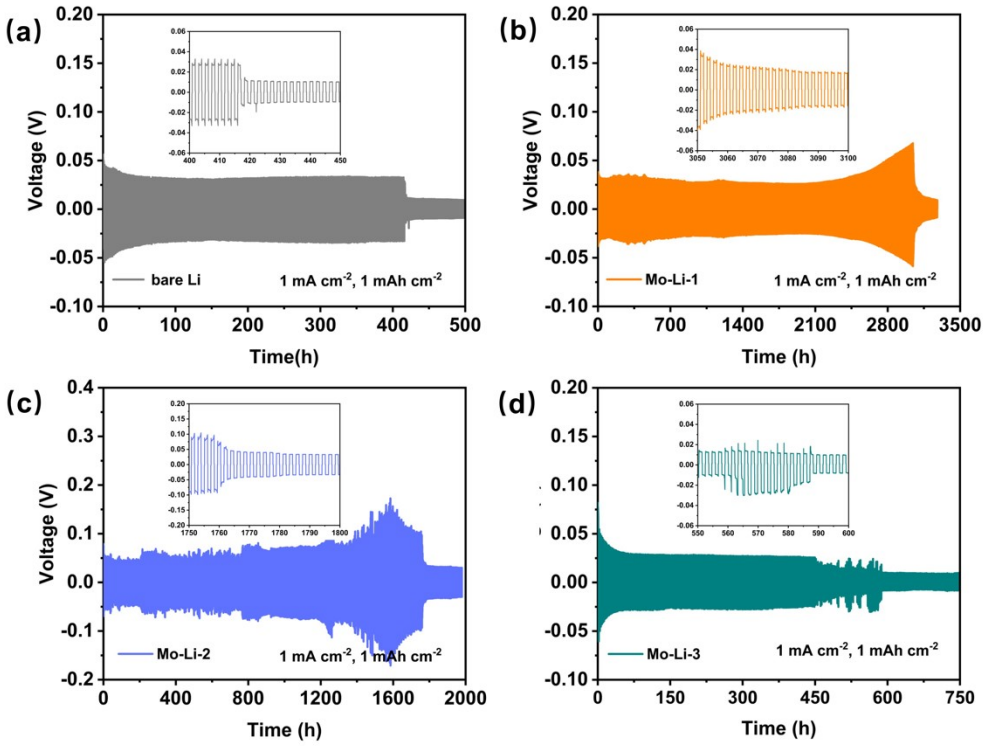


**Figure S9.** Voltage profiles of bare Li, Mo-Li-1, Mo-Li-2, and Mo-Li-3 anodes in symmetric cell at 1 mA $cm^{-2}$ for 1 mAh $cm^{-2}$. The insets of each image are enlarged voltage profiles near the end of the cycle life.

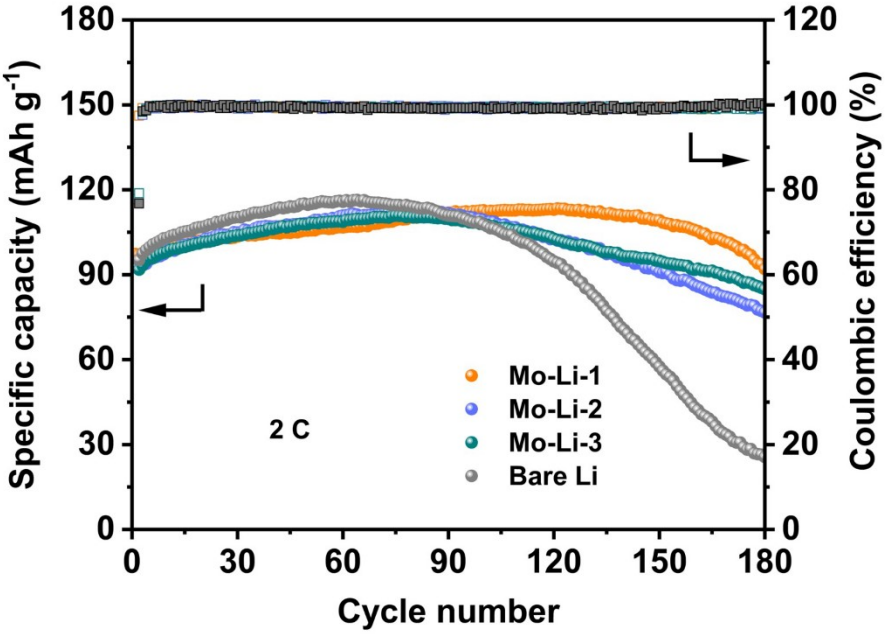


**Figure S10.** The long-term cycling of LFP full cells at 2C.

**Table S1.** The surface energy for the specific surface in the slab structures

| Mo content | Crystal face | Atom | $E_{slab}$（eV） | S (Å2) | γ （J $cm^{-2}$） |
|---|---|---|---|---|---|
| 0 | **Bare Li (110)** | 48 | -94.86 | 62.90 | 0.54 |
| 1/96 | **$Mo_1Li_{95}$ (110)** | 96 | -194.74 | 125.80 | 0.81 |
| 2/96 | **$Mo_2Li_{94}$ (110)** | 96 | -199.32 | 125.80 | 0.87 |
| 3/96 | **$Mo_3Li_{93}$ (110)** | 96 | -204.34 | 125.80 | 0.91 |
| 0 | **Bare Li (200)** | 48 | -92.72 | 88.91 | 0.58 |
| 1/96 | **$Mo_1Li_{95}$ (200)** | 96 | -190.30 | 177.82 | 0.77 |
| 2/96 | **$Mo_2Li_{94}$ (200)** | 96 | -200.58 | 177.82 | 0.56 |
| 3/96 | **$Mo_3Li_{93}$ (200)** | 96 | -206.33 | 177.82 | 0.54 |
| 0 | **Bare Li (211)** | 48 | -89.48 | 108.89 | 0.71 |
| 1/96 | **$Mo_1Li_{95}$ (211)** | 96 | -183.85 | 217.78 | 0.87 |
| 2/96 | **$Mo_2Li_{94}$ (211)** | 96 | -189.28 | 217.78 | 0.86 |
| 3/96 | **$Mo_3Li_{93}$ (211)** | 96 | -193.38 | 217.78 | 0.92 |

**Table S2.** The peak intensity ratio of various Li crystal faces.

| Sample | $I_{(110)}/I_{(200)}$ | $I_{(110)}/I_{(211)}$ | $I_{(200)}/_{(211)}$ |
|---|---|---|---|
| **Bare Li** | 2.37632275 | 8.64856914 | 3.6394758 |
| **Mo-Li-1** | 1.02877698 | 3.48780488 | 3.3902439 |
| **Mo-Li-2** | 0.59156555 | 4.86998402 | 8.23236577 |
| **Mo-Li-3** | 0.05720985 | 0.58353651 | 10.1999303 |